Power Electronic Systems
Laboratory

IEEE Transactions on Industrial Electronics, Vol. 66, No. 8, pp. 6404-6407, August 2019

A 300 000-r/min Magnetically Levitated Reaction Wheel Demonstrator

A. Tüysüz,
T. Achtnich,
C. Zwyssig,
J. W. Kolar

Eidgenössische Technische Hochschule Zürich
Swiss Federal Institute of Technology Zurich

A 300 000-r/min Magnetically Levitated Reaction Wheel Demonstrator

Arda Tüysüz, Timon Achtnich, Christof Zwyssig, *Member*, *IEEE*,
Johann W. Kolar, *Fellow Member*, *IEEE*

***Abstract*—Magnetic bearings can be used in reaction wheel systems to avoid several drawbacks of ball bearings, such as limited life time due to mechanical friction and lubricant monitoring/sealing requirements. Therefore, this letter discusses an electrical machine topology with integrated reaction wheel and magnetic bearings. The slotless/ironless structure, together with a new electromagnetic arrangement resulting in a shorter rotor than in earlier works, enables efficient operation at very high speeds, which in turn enables the miniaturization of the system. Measurements taken on a demonstrator prototype at 300 000 r/min show a significant increase of the feasible operational speed range compared to the state-of-the-art reaction wheels for small satellites, which typically run below 10 000 r/min.**

***Index Terms*—Bearingless Drive, High-Speed Drive, Magnetic Bearing, Reaction Wheel, Self-Bearing.**

I. Introduction

REACTION wheels (RWs) are key components of satellite attitude control systems [1], [2]. Due to their simplicity and compactness, ball bearings are commonly utilized for mounting RWs, especially in small satellites. However, ball bearings have several disadvantages. For instance, mechanical friction and wear limit the reliability and life time. Moreover, RWs with ball bearings usually require a sealed atmosphere in order to prevent the outgassing of the lubricant. Further disadvantages are stiction and a limited number of speed zero crossings (speed reversals) [3]. Magnetic bearings, due to their contactless operation and ability to work in vacuum, avoid all those drawbacks [4], [5]. Furthermore, an important source of microvibrations in satellites are the ball bearings, since they not only transfer the rotor imbalance forces to the satellite's chassis, but also generate microvibrations, e.g. due to the rolling of the balls and the motion of the bearing cage [6]. Those can also be avoided using magnetic bearings, since the rotor can be rotated around its center of mass, and the bearing force envelope can be actively controlled [7].

State-of-the-art RWs for small satellites typically run below $10\,000\,\mathrm{r/min}$ [8]. However, an initial study presented in [8] shows that their mass can be nearly halved by increasing their operating speeds from below $10\,000\,\mathrm{r/min}$ to $250\,000\,\mathrm{r/min}$.

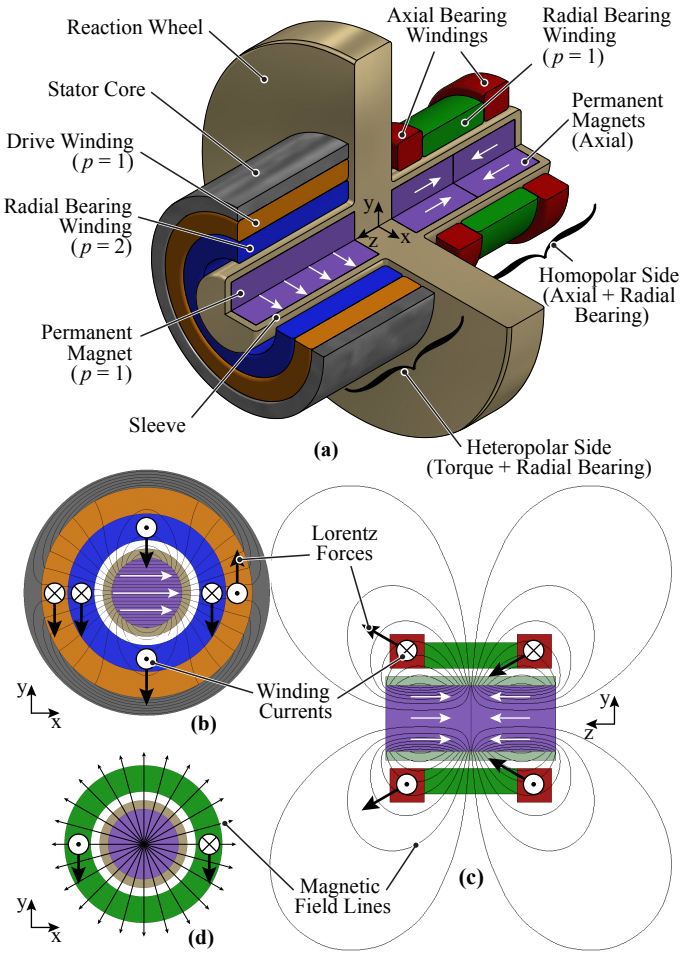

Fig. 1. (a) Three-quarter section view of the considered electrical machine with integrated magnetic bearings and RW. White arrows denote the magnetization direction of the PMs. (b) Cross-sectional view of the heteropolar side. The one-pole-pair PM field interacts with the one-pole-pair drive current to generate a torque, and with the two-pole-pair bearing current to generate a radial bearing force. (c) Cross-sectional view of the homopoloar side and the generation of the axial bearing force. (d) Cross-sectional view of the homopoloar side and the generation of the radial bearing force.

Manuscript received June 8, 2017; revised April 12, 2018; accepted July 3, 2018.

This work was supported financially by the State Secretariat for Education, Research and Innovation (SERI).

A. Tüysüz was with the Power Electronic Systems Laboratory, Swiss Federal Institute of Technology (ETH) Zurich, 8092 Zurich, Switzerland. He is now with ABB Corporate Research Center, 68526 Ladenburg, Germany (e-mail: arda.tueysuez@de.abb.com).

T. Achtnich and C. Zwyssig are with Celeroton Ltd., 8092 Zurich, Switzerland (e-mail: timon.achtnich@celeroton.com; christof.zwyssig@celeroton.com).

J. W. Kolar is with the Power Electronic Systems Laboratory, Swiss Federal Institute of Technology (ETH) Zurich, 8092 Zurich, Switzerland (e-mail: kolar@lem.ee.ethz.ch).

TABLE I
KEY PARAMETERS OF THE PROTOTYPE

Rotor axial length	49 mm	
Reaction wheel length	6 mm	
Reaction wheel diameter	30 mm	
Rotor (PM + sleeve) diameter	8 mm	
Reaction wheel axial moment of inertia	$2211\,\mathrm{g\,mm^2}$	
Angular momentum capacity	$69\,\mathrm{g\,m^2\,s^{-1}}$	
Sleeve and reaction wheel material	Titanium (grade 5)	
Stator core material	Amorphous iron	
Permanent magnet material	Sintered SmCo	
Drive winding	$1.01\,\Omega$	$39.5\,\mu\mathrm{H}$
Heteropolar radial bearing winding	$1.65\,\Omega$	$19.5\,\mu\mathrm{H}$
Homopolar radial bearing winding	$2.95\,\Omega$	$47.2\,\mu\mathrm{H}$
Axial bearing winding	$18.9\,\Omega$	$1.8\,\mathrm{mH}$

This is another major aspect where ball bearings impose limits that can be avoided by using magnetic bearings.

On the other hand, standalone magnetic bearings increase the total system size and complexity; and this has been limiting their use in small satellites. Therefore, a new electrical machine topology with integrated magnetic bearings and an integrated RW is presented in this letter. Measurements taken on a proof-of-concept demonstrator at speeds up to $300\,000\,\mathrm{r/min}$ show a significant increase of the feasible operational speed compared to the state-of-the-art RWs for small satellites, which typically run below $10\,000\,\mathrm{r/min}$.

II. ELECTRICAL MACHINE TOPOLOGY WITH INTEGRATED MAGNETIC BEARINGS AND REACTION WHEEL

The proposed dual hetero-/homopolar slotless/ironless self-bearing machine with integrated RW is shown in Fig. 1(a). Due to the slotless (heteropolar side) and ironless (homopolar side) structure, the operation of the machine can be easily explained by Lorentz forces. As depicted in Fig. 1(b), the one-pole-pair magnetic field of the rotor permanent magnet (PM) interacts with the three-phase, one-pole-pair currents in the drive winding to generate a torque; and with the three-phase, two-pole-pair currents in the bearing winding to generate a bearing force.

On the homopolar side, the two axially magnetized PMs are used to generate a homopolar magnetic field. The axial force is generated by coils wound in the azimuthal direction around the rotor, as shown in Fig. 1(c). It is to be noted that these coils should be placed to interact with mainly the radial component of the rotor field, in order to maximize the axial component of the Lorentz force. Finally, a radial force is generated on the homopolar side using a winding that is essentially the same as the drive winding, such that a one-pole-pair current would interact with the homopolar rotor field to create a bearing force (see Fig. 1(d)). Two PCB-based position sensors are used at both axial ends of the machine to measure the rotor position, whose placement can be seen in [8]. Tab. I summarizes the key parameters of the demonstrator prototype.

All six degrees of freedom are actively controlled in the proposed system by dedicated windings that produce a torque, an axial force and two radial forces acting on both sides. A

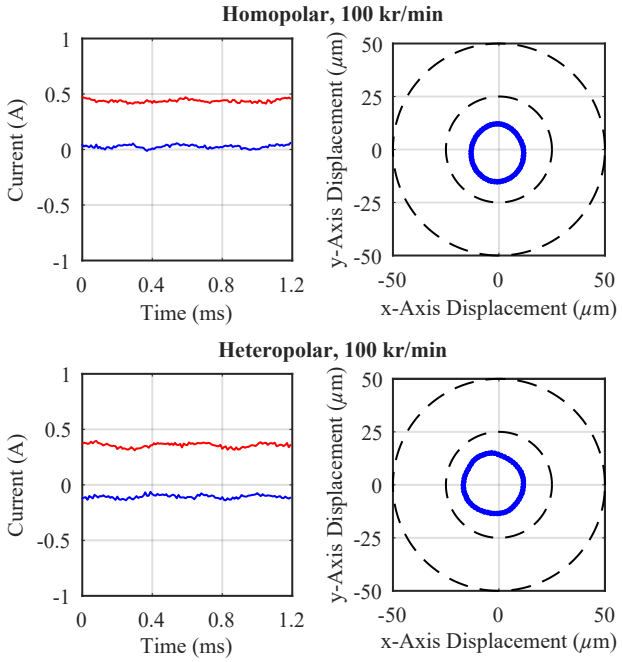

Fig. 2. Measured radial bearing currents and rotor displacements at $100\,000\,\mathrm{r/min}$, corresponding to rotational period of $0.6\,\mathrm{ms}$. The dq-frame is fixed to the rotor field rather than the rotor geometry, i.e., it rotates with the rotor on the heteropolar side, but is stationary on the homopolar side. Therefore, constant i_d (blue) and i_q (red) should be interpreted as three-phase sinusoidal currents in the heteropolar bearing. Contrarily, constant i_d and i_q means dc bearing currents in the homopolar side. Consequently, this convention means that the x- and y-direction components of the radial bearing forces are proportional to i_d and i_q, both for homopolar and heteropolar sides.

similar slotless, high-speed, self-bearing motor is shown in [9], where two heteropolar self-bearing motors and an additional axial bearing (PM and coil) are used. The concept proposed here, on the other hand, utilizes the axially magnetized PMs in the homopolar side for both axial and radial force generation, thereby leading to a shorter and rotor-dynamically more favorable rotor construction. Moreover, the load (the RW) is placed in the middle of the rotor, further increasing the critical speed of the first bending mode of the rotor [8]. SmCo is selected as the magnet material to prevent oxidation without coating the magnets, which is beneficial considering the tight mechanical tolerances. Moreover, its temperature stability allows a large operating temperature range.

In literature, disc-shaped (with short axial lengths and large diameters) self-bearing machines are shown to require only one drive and one radial bearing winding for stable operation, also at high-speeds [10]. However, the limited mechanical strength of the PMs limits the applicability of this machine type in RWs. Contrarily, the proposed topology allows for the independent dimensioning of the electrical machine/magnetic bearings and the RW, to ensure their best utilization (by having designs where both the PMs and RW are operated at their respective stress limits).

The implemented control strategy is discussed in [11], where the use of a notch filter is shown to suppress the magnetic bearing force for the rotor displacement caused by

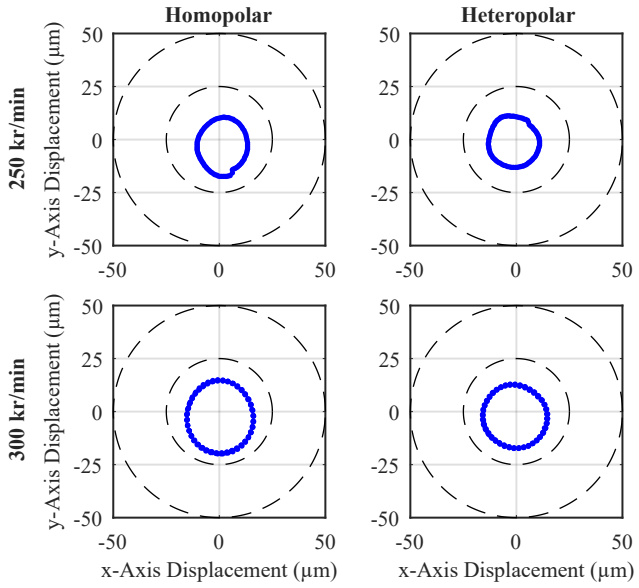

Fig. 3. Measured rotor displacements at $250\,000\,\mathrm{r/min}$ and $300\,000\,\mathrm{r/min}$. The fundamental frequency of both x- and y-displacements is the same as the rotational frequency.

unbalance, thereby allowing the rotor to rotate around its center of mass.

III. Measurement Results

Fig. 2 shows the measured radial bearing currents and rotor displacements at $100\,000\,\mathrm{r/min}$. It can be observed that the displacement is kept below $20\,\mu\mathrm{m}$. The constant position offset is due to the fixed-point implementation of the digital control; but it is not discussed further since it is rather small. The orbit of the rotor is clearly visible on both the homopolar and heteropolar sides, and is due to the mechanical unbalance.

The dc $i_{\mathrm{d,q}}$ currents show that the bearing force primarily counteracts the weight of the rotor, which is placed horizontally during measurements. The Joule losses in the homopolar and heteropolar bearing windings are $0.85\,\mathrm{W}$ and $0.35\,\mathrm{W}$, respectively; and these losses would tend towards zero while idling (even at high speeds) in a spacecraft not exposed to gravity. Fig. 3 shows the measured displacement at higher speeds, namely $250\,000\,\mathrm{r/min}$ and $300\,000\,\mathrm{r/min}$.

The axial displacement and the axial bearing current are plotted in Fig. 4 for $300\,000\,\mathrm{r/min}$. It can be seen the that the total axial displacement is kept below $\pm 50\,\mu\mathrm{m}$. The strongest frequency component in the axial displacement is the rotational frequency. The Joule losses in the axial bearing winding are negligible compared to the radial bearings.

In order to quantify the no-load losses of the considered electrical machine, the RW is first brought up to a certain high speed and then the drive power is cut off, and the speed profile is measured during deceleration. With the axial moment of inertia known, the braking torque and consequently the no-load losses of the machine are then calculated from this deceleration profile. Fig. 5 depicts both the deceleration profiles and the corresponding losses for operation under both vacuum and atmospheric air pressure. It can be seen clearly that the

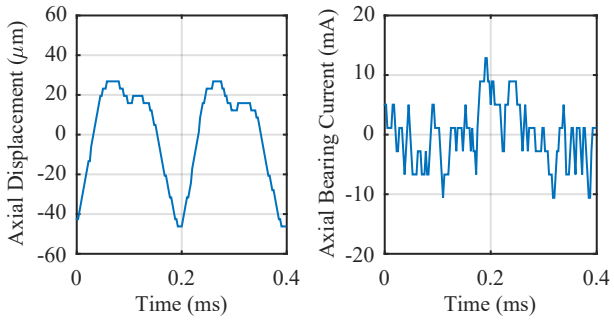

Fig. 4. Measured axial displacement and axial bearing current at $300\,000\,\mathrm{r/min}$. The dominant frequency component is the fundamental frequency of rotation.

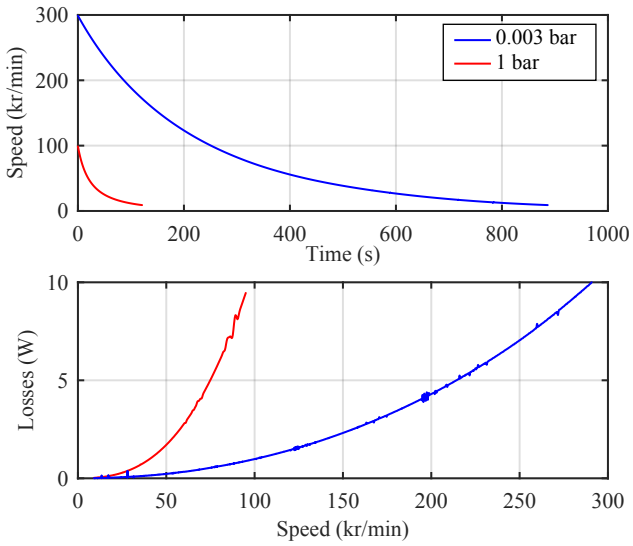

Fig. 5. Measured speed profiles during deceleration tests (top) and the resulting no-load losses (bottom) in vacuum and air atmosphere.

windage losses are rather high due to the large diameter of the RW; and they can be avoided when magnetic bearings are used as the they allow the RW to operate in vacuum.

Fig. 6 shows the back electro-motive force (EMF) of the drive winding, measured across two machine terminals. The flux linkage is calculated based on this measurement as $0.84\,\mathrm{mWb}$.

IV. Conclusion

Reaction wheels are widely used for attitude control of spacecraft with varying sizes and mission profiles. Today, especially in smaller satellites, ball bearings are the method of choice when it comes to rotor suspension, due to their compactness and simplicity. However, ball bearings exhibit unwanted friction and stiction, and they limit not only the life time and number of speed zero crossings but also the maximum operating speed of reaction wheels. Moreover, they are a major source of microvibrations, especially in small satellites. This letter discusses a new, self-bearing electrical machine with an integrated reaction wheel. Unlike systems

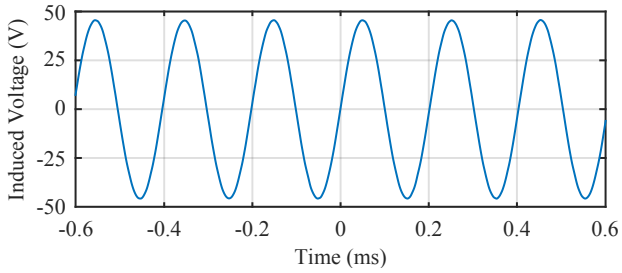

Fig. 6. Back EMF of the drive winding at $300\,000\,\mathrm{r/min}$, measured across two winding terminals (line to line).

with ball bearings, the considered system can run in vacuum, and can run at very high speeds, which allows for decreasing the overall reaction wheel system size. Measurements on a proof-of-concept demonstrator confirm feasible operation at speeds up to $300\,000\,\mathrm{r/min}$, which is around 30 times higher than that of the state-of-the-art reaction wheels for small satellites.

The future work shall focus on the design of a high signal-to-noise ratio drive/bearing inverter for investigating the microvibration reduction methods enabled by the magnetic bearings. Application-specific issues such as the fixation of the rotor during spacecraft launch via a launch lock, behavior during satellite power subsystem intermission, and the effect of the leakage magnetic field in terms of interference with neighboring systems or structures shall also be addressed in subsequent works.

REFERENCES

[1] B. Xiao, M. Huo, X. Yang and Y. Zhang, "Fault-Tolerant Attitude Stabilization for Satellites Without Rate Sensor," *IEEE Trans. Ind. Electron.*, vol. 62, no. 11, pp. 7191-7202, Nov. 2015.

[2] M. C. Chou and C. M. Liaw, "Dynamic Control and Diagnostic Friction Estimation for an SPMSM-Driven Satellite Reaction Wheel," *IEEE Trans. Ind. Electron.*, vol. 58, no. 10, pp. 4693-4707, Oct. 2011.

[3] B. Gerlach, M. Ehinger, H. K. Raue and R. Seiler, "Gimballing Magnetic Bearing Reaction Wheel with Digital Controller," *Euro. Space Mech. and Trib. Symp. (ESMATS)*, pp. 35-40, Sep. 2005.

[4] J. Tang, Z. Peng, B. Liu and K. Wang, "Control of Rotor's Vernier-Gimballing for a Magnetically Suspended Flywheel," *IEEE Trans. Ind. Electron.*, vol. 64, no. 4, pp. 2972-2981, Apr. 2017.

[5] J. Tang, K. Wang B. Xiang "Stable Control of High-Speed Rotor Suspended by Superconducting Magnetic Bearings and Active Magnetic Bearings," *IEEE Trans. Ind. Electron.*, vol. 64, no. 4, pp. 3319-3328, Apr. 2017.

[6] W. Ley, K. Wittmann and W. Hallmann, "Handbook of Space Technology," *John Wiley and Sons*, 2009.

[7] M. Kaufmann, A. Tüysüz, J. W. Kolar and C. Zwyssig, "High-Speed Magnetically Levitated Reaction Wheels for Small Satellites," *Int. Symp. Pow. Electron., Electr. Driv., Automat. Mot. (SPEEDAM)*, pp. 28-33, Jun. 2016.

[8] C. Zwyssig, T. Baumgartner and J. W. Kolar, "High-Speed Magnetically Levitated Reaction Wheel Demonstrator," *Int. Pow. Electron. Conf. (IPEC - ECCE Asia)*, pp. 1707-1714, May 2014.

[9] T. Baumgartner, R. M. Burkart and J. W. Kolar, "Analysis and Design of a 300-W 500 000-r/min Slotless Self-Bearing Permanent-Magnet Motor," *IEEE Trans. Ind. Electron.*, vol. 61, no. 8, pp. 4326-4336, Aug. 2014.

[10] H. Mitterhofer, W. Gruber and W. Amrhein, "On the High Speed Capacity of Bearingless Drives," *IEEE Trans. Ind. Electron.*, vol. 61, no. 6, pp. 3119-3126, Jun. 2014.

[11] T. Baumgartner and J. W. Kolar, "Multivariable State Feedback Control of a 500 000-r/min Self-Bearing Permanent-Magnet Motor," *IEEE/ASME Trans. on Mechatr.*, vol. 20, no. 3, pp. 1149-1159, Jun. 2015.